Phase diagram of hard-core bosons on a zigzag ladder

Davide Rossini, Valeria Lante, Alberto Parola, and Federico Becca

Phys. Rev. B **83**, 155106 — Published 7 April 2011

DOI: 10.1103/PhysRevB.83.155106

Phase diagram of hard-core bosons on a zig-zag ladder

Davide Rossini
NEST, Scuola Normale Superiore & Istituto di Nanoscienze - CNR, Piazza dei Cavalieri 7, I-56126 Pisa, Italy

Valeria Lante and Alberto Parola
Dipartimento di Fisica e Matematica, Università dell'Insubria, Via Valleggio 11, I-22100 Como, Italy

Federico Becca
Democritos Simulation Center CNR-IOM Istituto Officina dei Materiali, Via Bonomea 265, I-34136, Trieste, Italy
(Dated: February 24, 2011)

We study hard-core bosons with unfrustrated nearest-neighbor hopping t and repulsive interaction V on a zig-zag ladder. As a function of the boson density ρ and V/t, the ground state displays different quantum phases. A standard one-component Tomonaga-Luttinger liquid is stable for $\rho < 1/3$ (and $\rho > 2/3$) at any value of V/t. At commensurate densities $\rho = 1/3$, $1/2$, and $2/3$ insulating (crystalline) phases are stabilized for a sufficiently large interaction V. For intermediate densities $1/3 < \rho < 2/3$ and large V/t, the ground state shows a clear evidence of a bound state of two bosons, implying gapped single-particle excitations but gapless excitations of boson pairs. These properties can be understood by the fact that the antisimmetric sector acquires a gap and a single gapless mode survives. Finally, for the same range of boson densities and weak interactions, the system is again a one-component Tomonaga-Luttinger liquid with no evidence of any breaking of discrete symmetries, in contrast to the frustrated case, where a $\mathcal{Z}_2$ symmetry breaking has been predicted.

PACS numbers: 75.10.-b, 75.10.Pq, 05.30.Jp, 71.30.+h

I. INTRODUCTION

Quantum many-body systems can give rise to remarkable collective states of matter that have no counterpart in their classical analogs. Archetypal examples include superfluids, superconductors, and insulating quantum liquids that play a major role in modern Condensed Matter and Materials Science. However, collective quantum phenomena are also ubiquitous in other contexts, like Nuclear Physics, Quantum Chemistry, and Atomic Physics. In particular, ultra-cold atoms loaded into optical lattices provide a unique possibility for engineering quantum systems with a very high degree of tunability and control of the experimental parameters.[1] They allow the realization of "quantum simulators" for ideal Condensed Matter models, which may provide answers to fundamental questions.[2] The first striking demonstration in this direction has been the observation of the superfluid to Mott insulator transition for bosons with short-range interactions;[3] more recently, a fermionic Mott insulator has been also observed.[4] Theoretical progresses and experimental achievements steadily open new research directions. Highly non-trivial phenomena and very rich phase diagrams are now conceivable by considering further ingredients, like long-range interactions, spin or multi-species models, frustration, and disorder.

Cold gases of bosonic particles trapped in optical lattices may be very well described by simple Bose-Hubbard models,[5] which contain hopping and short-range interaction terms.[6,7] Models of strongly-interacting bosons in one-dimensional (1D) or quasi-1D lattices constitute important examples where unconventional phases can be stabilized at low temperature. These systems do not represent a purely abstract problem, since it is now possible to confine the atomic species in almost decoupled 1D tubes, with[8] or without[9] an optical lattice. In realistic experimental setups, beyond pure 1D systems, the case of a two-leg ladder is very easy to obtain. Indeed, one can realize a double-well potential along a direction (say, y) like in Ref. 10, and a potential creating a cigar geometry in the x-axis. Then, by superimposing a further periodic potential along x, one realizes a two-leg Hubbard model. By playing with the distance between tubes and the height of the barrier between the two legs, one could tune the hopping rate between the legs. Likewise, the intra-chain hopping rate can be tuned by appropriately setting the strength of the periodic potential along the x direction.

Recent experimental results have driven a new impetus to understand their relevant low-energy properties. In particular, the study of quasi-1D systems, e.g., ladders, may be very important, in order to elucidate the nature of exotic quantum phases that escape the standard Tomonaga-Luttinger theory.[11] From a theoretical point of view, ladders are quasi-one-dimensional systems. For this kind of anisotropic systems, very efficient and accurate numerical methods have been also developed in the last 20 years, like exact diagonalizations by the Lanczos technique[12], or the density-matrix renormalization group (DMRG) method.[13] Within these approaches, it is possible to have numerically exact results on fairly large clusters, so to have insights into the physical properties at the thermodynamic limit. Moreover, in 1D systems a clear theoretical framework is provided by the bosoniza-

tion method,[11] which is helpful for classifying the possible phases.

In the following, we will consider a zig-zag ladder with two legs, which is topologically equivalent to a 1D lattice with equal nearest and next-nearest neighbor hopping and interaction, see Fig. 1. We will study the case of hard-core bosons that interact through a nearest-neighbor potential:

$$\mathcal{H} = -t \sum_{\langle i,j \rangle} (b_i^\dagger b_j + h.c.) + V \sum_{\langle i,j \rangle} n_i n_j, \qquad (1)$$

where $\langle i,j \rangle$ indicate nearest-neighbor sites in the zig-zag geometry of Fig. 1, $b_i^\dagger$ (b_i) creates (destroys) a boson on the site i and $n_i = b_i^\dagger b_i$ is the boson density. The hard-core constraint is imposed via the additional requirement $n_i = 0, 1$ on each site. The number of sites and bosons will be denoted by L and M, respectively; the boson density is $\rho = M/L$. In the following, we will focus on the case of unfrustrated hopping, i.e., $t > 0$.

We mention that the Hamiltonian (1) maps onto a system of $S = 1/2$ spins ($S_i^z = n_i - 1/2$) with antiferromagnetic coupling $J^z = V$ between the z components of spins and super-exchange $J^{xy} = -2t$ between their x and y components. Previous works have been focused on the case with negative hoppings, i.e., $t < 0$, that corresponds to an antiferromagnetic Heisenberg model. In particular, the one-dimensional chain with SU(2) symmetry (i.e., $V = 2|t|$) but different nearest- (J_1) and next-nearest-neighbor (J_2) interactions has been widely discussed, also in presence of a finite magnetic field.[14–16] On the other hand, here we are interested in the case with positive hopping parameters and $V > 2t$, in order to describe strongly interacting bosons in low-dimensional systems that are relevant for atomic gases trapped in optical lattices. However, we will show that some features of the phase diagram do not depend upon the sign of t and can be understood on the basis of the strong-coupling (classical) limit $V/t \to \infty$.

For future reference, it is useful to point out that in lattices where each site has the same coordination number z (equal to the number of neighbors), the microscopic model is invariant under "particle-hole symmetry", defined as the spin rotation of an angle π around the x-axis. This particle-hole transformation, which is indeed a canonical transformation due to the hard-core constraint, allows one to relate the full energy spectrum at different densities:

$$E(L-M) = E(M) + \frac{Vz}{2}(L - 2M) \qquad (2)$$

giving rise to a phase diagram symmetrical across the line $\rho = 1/2$. Open-boundary conditions violate this symmetry leading to specific finite-size effects, since a few sites have a smaller coordination number. In the following, open-boundary conditions will be used in DMRG, while periodic boundary conditions will be adopted in Lanczos calculations.

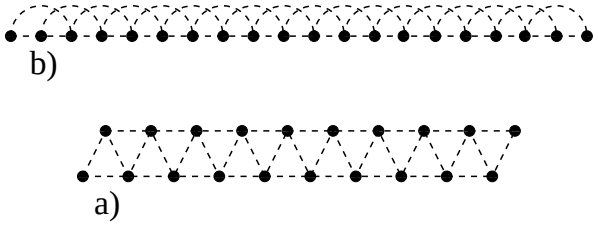

FIG. 1: The two-leg ladder (a) is topologically equivalent to a one-dimensional chain with nearest and next-nearest connections (b).

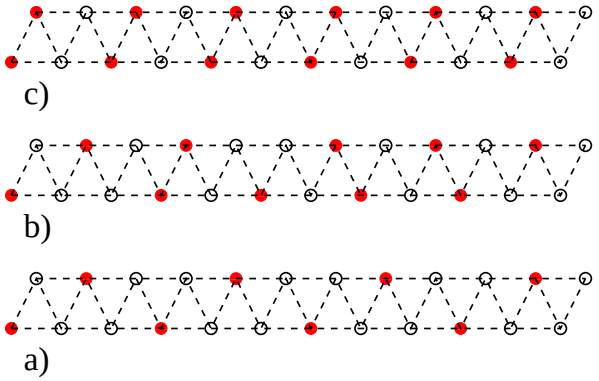

FIG. 2: (Color online) Examples of classical ground states for different boson densities. Full (empty) circles indicate particles (empty sites). (a) $\rho = 1/3$, where the ground state is three-fold degenerated; (b) $1/3 < \rho < 1/2$, where the ground state has a finite entropy; (c) $\rho = 1/2$, where the ground state is four-fold degenerated and corresponds to pairs of nearest-neighbor particles.

The paper is organized as follows: in Sec. II, we illustrate some useful preliminary consideration related to the classical limit of $t = 0$; in Sec. III, we present our numerical results; finally, in Sec. IV, we draw our conclusions.

II. PRELIMINARY CONSIDERATIONS

Before presenting our numerical results, we would like to discuss in some detail the classical limit of $t = 0$, which is relevant for the physical properties in the strong-coupling regime, i.e., $V/t \gg 1$. Let us take for convenience $L = 3 \times n$ with n multiple of 4 and quantize the q vectors as $q = \frac{2\pi}{L}k$, with $k = 0, \ldots, L-1$. Whenever the number of bosons $M < n$, i.e., $\rho = M/L < 1/3$, the classical ground state has zero energy and finite entropy. A finite value of t/V will drive the system towards a Tomonaga-Luttinger liquid with long-range charge-density-waves or superfluid correlations. Exactly at $M = n$ (namely $\rho = 1/3$) a commensurate density wave of longitudinal wave-vector $q = 2\pi/3$ sets in, leading to a three-fold degenerate solid-like ground state, as shown in Fig. 2(a). The energy gap is proportional to V

and, therefore, this insulating state is expected to remain stable also in presence of a small hopping parameter (see below, our numerical results). By further adding bosons, we find that for any density of the form $M = n + 2\delta$, with δ equal to an integer smaller than $n/4$ (so that $1/3 < \rho < 1/2$), the ground state is highly degenerate and still gapped, with energy $E = 3V\delta$ and single particle gap $E(M+1) - E(M) = 2V$. All possible ground states may be obtained by viewing the state, in the one dimensional topology, as a mixture of single particles and nearest-neighbor pairs, and placing these objects on the lattice in such a way that the nearest-neighbor sites of each object are empty, see Fig. 2(b). Given the huge degeneracy of all these classical states, a finite value of t has a dramatic effect, as it will be shown in the next section. Note that for these densities the binding energy $\Delta = E(M) + E(M+2) - 2\,E(M+1)$ is negative (i.e., $\Delta = -V$) implying the formation of boson pairs in the model. Finally, for $\rho = 1/2$, only nearest-neighbor pairs are present and the ground state is a four-fold degenerate gapped "molecular solid" characterized by a crystal ordering with longitudinal wave-vector $q = \pi/2$, see Fig. 2(c).

These results for the two-leg ladder in the classical limit can be conveniently summarized by considering the boson density ρ as a function of the chemical potential μ: at $\mu = 0$, the density jumps from $\rho = 0$ to $\rho = 1/3$, where it displays a plateau up to $\mu = 3V/2$. Then, the density jumps again to $\rho = 1/2$ and then remains constant up to $\mu = 5V/2$. A density discontinuity from $\rho = 1/2$ to $\rho = 2/3$ is followed by a plateau to $\mu = 4V$ where ρ jumps again to its limiting value $\rho = 1$. Therefore, in the classical limit, the model displays three distinct gapped (solid) phases of density $\rho = 1/3$, $1/2$, and $2/3$, besides the trivial "empty" ($\rho = 0$) and "full" ($\rho = 1$) states. At intermediate densities phase coexistence between neighboring phases sets in. As we will see in the next paragraph, a finite value of t removes this coexistence by favoring stable phases. In particular, for $1/3 < \rho < 1/2$, long-range charge-density-wave correlations develop at an incommensurate wave-vector q, which smoothly interpolates between the two limiting values ($q = 2\pi/3$ for $\rho = 1/3$, and $q = \pi/2$ for $\rho = 1/2$) characterizing the two solids at coexistence for $t = 0$.

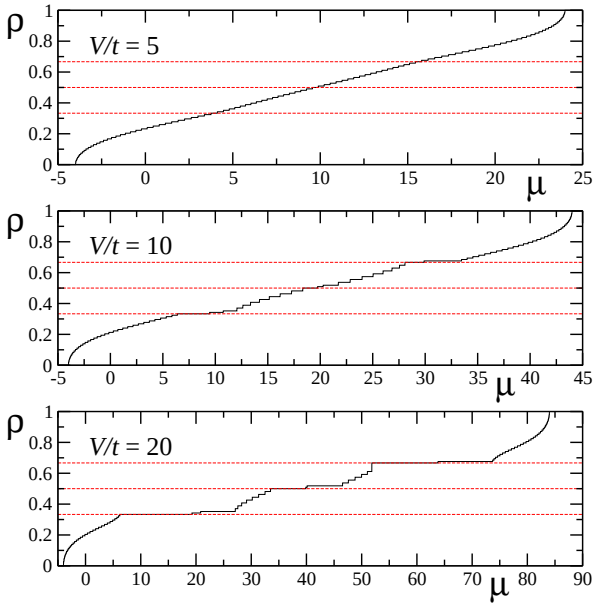

FIG. 3: (Color online) Boson density ρ as a function of the chemical potential μ for three different values of the interaction V/t. Calculations have been done on a lattice with $L = 108$ sites and open boundary conditions.

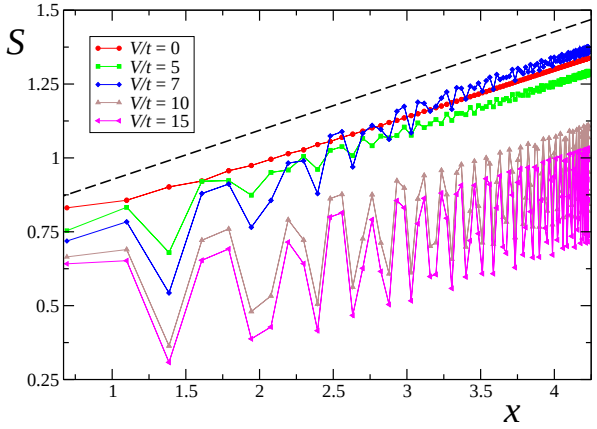

FIG. 4: (Color online) Entanglement entropy S as a function of the (reduced) block length x, for $\rho = 5/12$ and for different values of the interaction strength V/t. The dashed line indicates the slope 1/6 (equivalent to $c = 1$). The number of sites is $L = 216$.

III. RESULTS

Here, we present our numerical results on the two-leg ladder. The standard finite-size DMRG algorithm has been adopted,[13] fixing the total number of sites L and bosons M. Systems of up to $L = 216$ sites have been simulated, keeping $m \sim 300$ states and performing $n_{sw} \sim 6$ sweeps, in order to reach convergence both in the energies and in the measure of observables. Open-boundary conditions have been used, see Fig. 1(b). The latter choice determines small asymmetries in the phase diagram when comparing ρ and $(1-\rho)$, which vanish in the thermodynamic limit. In addition, DMRG results have been compared to Lanczos diagonalizations up to $L = 36$ sites with periodic boundary conditions.

In Fig. 3, we report the behavior of the boson density ρ as a function of the chemical potential μ: for each μ, the corresponding density $\rho = M/L$ is obtained by minimizing the free energy $E(M) - \mu M$ with respect to M. For small interactions, on any finite size, $\rho(\mu)$ displays small steps for every value of M; therefore, the ground state is always gapless, the density being a smooth function of the chemical potential μ. For $\rho < 1/3$

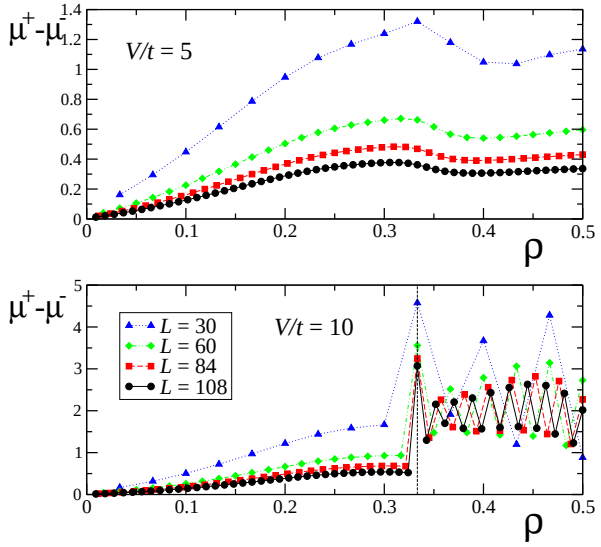

FIG. 5: (Color online) Difference between the energy needed to add a particle $\mu^+ = E(M+1) - E(M)$ and the one needed to remove it $\mu^- = E(M) - E(M-1)$ (where $E(M)$ is the energy of M particles) as a function of the density ρ, for different sizes of a system with $V/t = 5$ (upper panel) and $V/t = 10$ (lower panel).

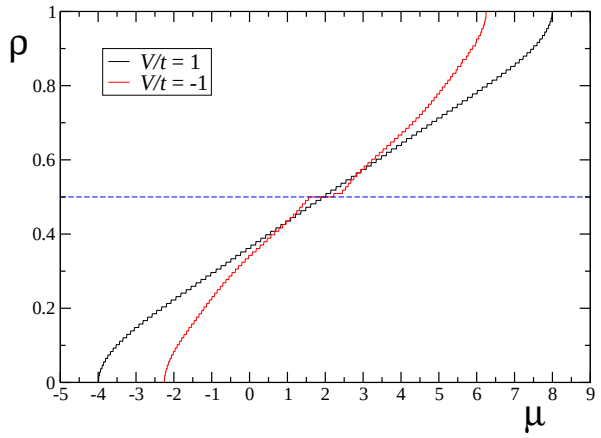

FIG. 6: (Color online) Boson density ρ as a function of the chemical potential μ for positive and negative values of the hopping parameters. Calculations have been done on a system with $L = 108$ sites with open boundary conditions. The existence of a plateau at $\rho = 1/2$ is clear for $t = -1$, whereas no plateau is present for $t = 1$.

(and $\rho > 2/3$), the system can be described by a one-component Tomonaga-Luttinger liquid, where the low-energy excitations are free massless bosons (ϕ, θ) and its central charge is $c = 1$.[11] The latter quantity can be numerically measured through the entanglement entropy:

$$S(l) = -\mathrm{Tr}_\Omega \left[\rho_{rdm}(l) \ln \rho_{rdm}(l)\right], \tag{3}$$

where $\rho_{rdm}(l)$ is the reduced density matrix for the subsystem Ω, containing all the sites from 1 to l, and is defined by:

$$\rho_{rdm}(l) = \mathrm{Tr}_{\bar{\Omega}} |\Psi_0\rangle\langle\Psi_0|. \tag{4}$$

Here $|\Psi_0\rangle$ is the ground state wave function and $\bar{\Omega}$ defines the environment (all sites from $l+1$ to L). The central charge can be obtained from the logarithmic divergence of $S(l)$:[17,18]

$$S(l) = \frac{c}{6} \ln l + \ldots, \tag{5}$$

which is valid in the thermodynamic limit and $l \gg 1$. In finite systems, it is useful to consider:[16]

$$x = \ln \left[\frac{L}{\pi} \sin\left(\frac{\pi l}{L}\right)\right], \tag{6}$$

instead of $\ln l$. Since the reduced density matrix $\rho_{rdm}(l)$ is directly available by DMRG calculations, the central charge c can be easily computed, by fitting the linear slope of $S(l)$ as a function of x. We verified that $c = 1$ in the low-density regime $\rho < 1/3$ and at any interaction strength.

The intermediate boson density at weak coupling requires a deeper discussion. Indeed, a naive analysis based upon the band structure (and the connection to spin-less fermions through the Jordan-Wigner transformation[19]) would suggest that the low-energy physics is described by a two-component Tomonaga-Luttinger liquid, with $c = 2$. However, we find that $c = 1$ also in this regime, see Fig. 4. The limiting case with $V = 0$ corresponds to "non-interacting" hard-core bosons with unfrustrated hopping amplitude, which are expected to give rise to a standard quasi-condensed quantum liquid. Therefore, spin-less fermions and hard-core bosons are inherently different in this regime of densities (e.g., the Jordan-Wigner string caused by hopping along the legs plays a relevant role in this zig-zag geometry). We mention that in the case with frustrated hopping (equivalent to the antiferromagnetic spin XY model), the ground state is expected to develop a chiral order that breaks a discrete $\mathcal{Z}_2$ symmetry.[20,21] Similarly, a chiral phase has been also predicted for isotropic frustrated spin chains in presence of a magnetic field.[16,22,23] On the contrary, for our unfrustrated model, we do not find any evidence of symmetry breaking for $V \geq 0$, as can be seen from Lanczos spectra at low-energy (not shown). Therefore, we conclude that there is a fundamental difference between frustrated and unfrustrated bosons at these densities: for the former case, a gapless state with broken $\mathcal{Z}_2$ symmetry is expected, while, in the latter one, a pure gapless Tomonaga-Luttinger liquid is realized.

By increasing the ratio V/t, two plateaus emerge at $\rho = 1/3$ and $2/3$, for $V/t \gtrsim 8$, indicating the stabilization of insulating phases with a finite excitation gap, see Fig. 3. These states can be adiabatically connected to the solid phases that have been discussed in Sec. II. Remarkably, the stabilization of crystalline phases at commensurate fillings is accompanied by a significant modification of the intermediate phase at $1/3 < \rho < 2/3$.

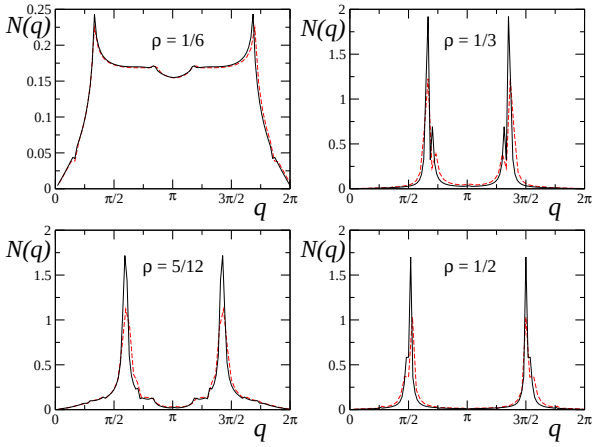

FIG. 7: (Color online) Density structure factor $N(q)$ for different boson densities. Calculations have been done on lattices with $L = 108$ (solid curves) and $L = 60$ (dashed curves) for $V/t = 20$.

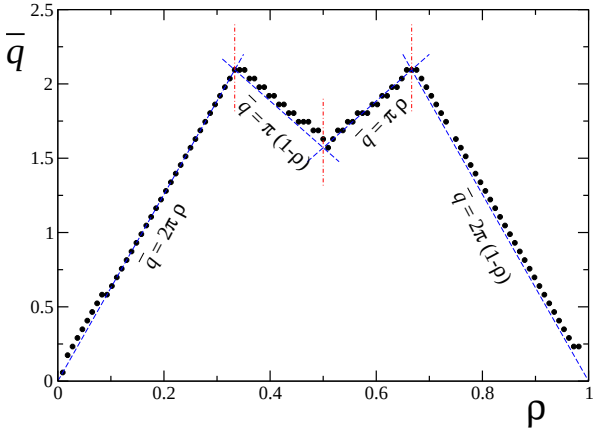

FIG. 8: (Color online) Position of the peak $\bar{q}$ of the density-density correlations as a function of the density. The value of $\bar{q}$ does not depend upon the interaction strength V/t.

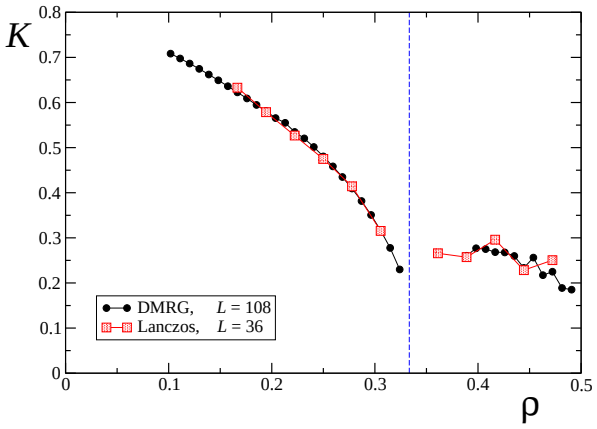

FIG. 9: (Color online) Tomonaga-Luttinger parameter K as a function of the boson density ρ for $V/t = 10$.

Indeed, whereas for $V/t \lesssim 8$ the liquid phase displays a standard gapless behavior, with a vanishing excitation energy when adding or removing a single boson, the strong-coupling phase is instead gapped for single-particle excitations, as clearly shown in Fig. 5, where the difference between $\mu^+ = E(M+1) - E(M)$ and $\mu^- = E(M) - E(M-1)$ is reported. In the strong-coupling regime, for $\rho < 1/3$, $\mu^+ - \mu^-$ is a smooth function of ρ that goes to zero in the thermodynamic limit, while for intermediate densities, this quantity remains finite, indicating the presence of a finite gap in the single-particle excitations. However, such a strong-coupling phase is not insulating, since excitations of pairs of bosons are still gapless. The plot of $\rho(\mu)$ shown in Fig. 3 supports this interpretation showing that, on any finite-size system, steps twice as big as in the standard Tomonaga-Luttinger liquid occur. The emergence of the two-boson bound state is simply due to a potential energy gain and does not depend on the sign of t: as previously noticed, even in the classical limit ($t = 0$), the binding energy $\Delta = E(M) + E(M+2) - 2\,E(M+1)$ is negative in this part of the phase diagram (see Sec. II). Not surprisingly, a similar behavior has been also found in the J_1-J_2 Heisenberg model in presence of a magnetic field.[15,16,24] In spin systems, the effect, which was called "even-odd", is characterized by the existence of two-magnon excitations in the region of weakly coupled antiferromagnetic chains. This phase may be described by a low-energy theory with two bosonic fields (ϕ_n, θ_n), with $n = 1, 2$, which give rise to symmetric and antisymmetric combinations; the presence of relevant interactions leads to the opening of an energy gap in the antisymmetric channel, implying a two-boson bound state.[15,16] A similar mechanism has been also discussed in the study of a frustrated spin-1/2 zig-zag ladder with ferromagnetic nearest-neighbor and antiferromagnetic next-nearest-neighbor interactions.[25–27]

We would like to mention that the solid at $\rho = 1/2$ appears to be less stable than the other two at 1/3 and 2/3. Indeed, we start to detect its existence for $V/t = 10 \div 11$, although the width of the plateau in a $\rho(\mu)$ plot is still fairly small. In Fig. 3, we show that eventually a clearly insulating phase exists for $V/t = 20$. On the contrary, a very stable solid phase for $\rho = 1/2$ may be obtained by changing sign of the hopping parameters; in this case, the model is equivalent to the anisotropic J_1-J_2 Heisenberg chain, which shows a dimerized phase at zero magnetization.[28,29] In Fig. 6, we report a comparison of $\rho(\mu)$ for positive and negative hopping parameters and $V/|t| = 1$. Only when $t = -1$ a clear plateau is present, indicating that change in the sign of the hopping parameters has a dramatic effect in the stabilization of the insulating phase at half filling.

The nature of the ground state can be better characterized by studying the density-density correlation function. In the case with open-boundary conditions, used within

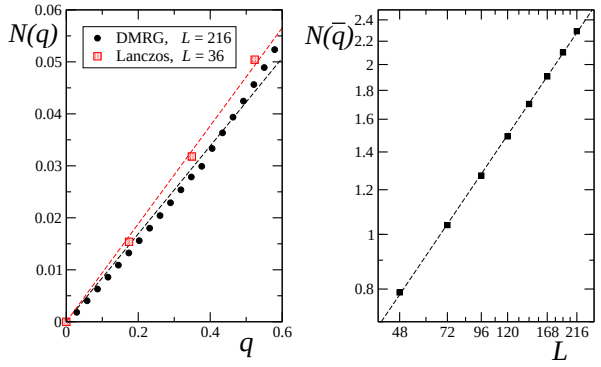

FIG. 10: (Color online) DMRG results for the density-density correlation functions on systems with open boundary conditions. Left panel: small-q behavior of $N(q)$ for a 216-site system. Data for 36 sites with periodic boundary conditions obtained by Lanczos diagonalizations are also shown. The boson density is $\rho = 5/12$, while $V/t = 10$. A linear fit of numerical DMRG data gives $K = 0.27 \pm 0.01$, while for Lanczos data $K = 0.29 \pm 0.02$. Apart from the system sizes, the small discrepancies could be ascribed to different boundary conditions imposed in the two cases. Right panel: size scaling of the peak of the structure factor $N(\bar{q}) \propto L^{\alpha}$. The exponent $\alpha = 0.71 \pm 0.01$ is in good agreement with the value $1 - K$ obtained from the previous fits. Dashed lines are fits of the numerical results.

DMRG calculations, we define:

$$N(r, r') = \langle n_r n_{r'} \rangle - \langle n_r \rangle \langle n_{r'} \rangle, \qquad (7)$$

which depends separately on r and r'. It is convenient to perform the Fourier transform

$$N(q) = \frac{2}{L+1} \sum_{r,r'} \sin(q\, r) \sin(q\, r') N(r, r'), \qquad (8)$$

with $q = 2\pi n/(L+1)$ and $n = 1, \ldots, L$. With periodic-boundary conditions, implemented with Lanczos algorithm, correlation functions only depend upon the distance $|r - r'|$, and the standard Fourier transform can be employed. In Fig. 7, we show the behavior of the density structure factor $N(q)$ at $V/t = 20$ for different densities. For $\rho < 1/3$, the ground state is described by a standard one-component Tomonaga-Luttinger liquid, for which (in a translationally invariant system):[11,16]

$$\langle n_r n_0 \rangle = \rho^2 - \frac{K}{2\pi^2 r^2} + A \frac{\cos(2\pi\rho\, r)}{r^{2K}} + \ldots \qquad (9)$$

where A is a numerical constant and K is the Tomonaga-Luttinger parameter that describes the low-energy model.[11] $N(q)$ displays a peak at $\bar{q} = 2\pi\rho$ (see Fig. 8), in agreement with a single-band picture with $k_F = \pi\rho$. No long-range order is implied, since the finite-size peak grows slower than L: $N(\bar{q}) \sim L^{1-2K}$. The one particle density matrix decays as $1/r^{1/2K}$. Therefore, the dominant correlations have a charge-density wave (CDW) character for $K < 1/2$, while for $K > 1/2$ a divergence in the $q = 0$ occupation number occurs (i.e., quasi-condensation).

A convenient way to compute the Tomonaga-Luttinger parameter K is via the small-q behavior of $N(q)$. From Eq. (9) we easily obtain $N(q) = \frac{K}{2\pi}\, q$. In Fig. 9, we report the resulting K as a function of the density ρ for $V/t = 10$ (also obtained by Lanczos diagonalizations on $L = 36$ sites). At low density, bosons are in a quasi-condensed state but, close to quarter filling, the crossover to a CDW phase takes place.

At the commensurate density $\rho = 1/3$ and sufficiently large V/t, true long-range order sets in and $N(\bar{q}) \sim L$, together with a quadratic behavior of $N(q)$ at small momenta, i.e., $N(q) \sim q^2$. When approaching $\rho = 1/3$ by varying the boson density, the parameter K is expected to remain finite, with a value that does not depend upon the interaction strength and is twice the limiting value obtained at constant density ($\rho = 1/3$) when V/t tends to the transition value from below.[30] We mention that, in the classical limit $t = 0$ by using the results of Ref. 31, we find that $K = 1/9$ for $\rho \to 1/3$, which may be compatible with the strong renormalization that is observed in our numerical results for $V/t = 10$ when approaching the insulating phase, see Fig. 9.

For intermediate boson densities, i.e., $1/3 < \rho < 1/2$, the presence of strong interactions open a gap in the antisymmetric channel, leading to an effective one-component Tomonaga Luttinger model. In this case, we have:[16]

$$\langle n_r n_0 \rangle = \rho^2 - \frac{K}{\pi^2 r^2} + A' \frac{\cos[\pi(1-\rho)\, r]}{r^K} + \ldots \qquad (10)$$

where A' is a numerical constant and K is the Tomonaga-Luttinger parameter in the effective low-energy model of the gapless bosonic field. Pair condensation can be investigated trough the correlation function[16]

$$\langle b_r^\dagger b_{r+1}^\dagger b_0 b_1 \rangle = \frac{B}{r^{1/K}} + \ldots \qquad (11)$$

where B is a numerical constant. In this regime, $N(q) = \frac{K}{\pi} q$ and the peak of the structure factor shifts to $\bar{q} = \pi(1-\rho)$, see Fig. 8. Again there is no true long-range order, since $N(\bar{q})$ diverges as L^{1-K}. By fitting the small-q part of the structure factor, we are able to extract the behavior of K also in this part of the phase diagram, see Fig. 9 for the case of $V/t = 10$. A fairly good agreement is obtained by comparing the power law divergence of the peak in $N(q)$ with the expected exponent $1 - K$. In Fig. 10, we report these results for $\rho = 5/12$ and $V/t = 10$. In this phase, CDW correlations dominate and coexist with power-law pairing correlations, which however do not lead to (quasi) pair condensation because $K < 1$ in the whole density interval.

Finally, for $\rho = 1/2$ and large V/t, the ground state has again crystalline order with $N(\bar{q}) \sim L$ and $N(q) \sim q^2$.

IV. CONCLUSIONS

In this paper, we have studied hard-core bosons with unfrustrated hopping and nearest-neighbor interaction on a zig-zag ladder. For small V/t, the ground state is a gapless Tomonaga-Luttinger liquid for all densities. For $\rho < 1/3$ (and $\rho > 2/3$), the density-density correlations have a peak for $\bar{q} = 2\pi\rho$. This fact suggests that a fermionic band picture (originating from the standard Jordan-Wigner transformation) is correct and the Jordan-Wigner string is a small perturbation to free spinless fermions. For intermediate densities $1/3 < \rho < 2/3$, $N(q)$ shows a peak at $\bar{q} = \pi(1-\rho)$, still having one gapless mode and central charge $c = 1$. This fact contrasts the naive expectation based upon the Jordan-Wigner transformation, which would suggest the presence of a two-component Luttinger liquid phase with $c = 2$. Moreover, we do not find any evidence of discrete $\mathcal{Z}_2$ symmetry breaking, as found in the case with frustrated hopping.[20,21] In our case, for weak interactions, the ground state is a pure quantum liquid, with a single gapless mode. By increasing V/t, three solid phases appear at commensurate boson densities, first at $\rho = 1/3$ and $2/3$ (for $V/t \simeq 8$) and then at $\rho = 1/2$ (for $V/t \simeq 10$): these are insulating phases with long-range order in the density profile. For $1/3 < \rho < 2/3$ there is CDW phase, which has gapped single-particle excitations but gapless excitations for pairs of bosons. This phase, which has been also found in frustrated antiferromagnetic spin models, can be described by a one-component Tomonaga-Luttinger model, where the antisymmetric sector acquires a finite gap from the (large) interaction V/t.

Acknowledgments

We thank M. Fabrizio for many important discussions during the whole duration of the project. F.B. also thanks T. Giamarchi for interesting suggestions in Santa Barbara, during the program "Disentangling Quantum Many-body Systems: Computational and Conceptual Approaches". F.B. wants to acknowledge the fact that this research was supported in part by the National Science Foundation under the Grant No. NSF PHY05-51164. D.R. acknowledges support from EU through the project SOLID, under the grant agreement No. 248629. The DMRG code released within the PwP project (www.dmrg.it) has been used.

[1] I. Bloch, J. Dalibard, and W. Zwerger, Rev. Mod. Phys. **80**, 885 (2008)

[2] For a recent review of cold atomic gases in optical lattices, see for example, M. Lewenstein, A. Sanpera, V. Ahufinger, B. Damski, A. Sen De, and U. Sen, Adv. Phys. **56**, 243 (2007).

[3] M. Greiner, O. Mandel, T. Esslinger, T.W. Hansch, I. Bloch, Nature (London) **415**, 39 (2002).

[4] R. Jordens, N. Strohmaier, K. Gunter, H. Moritz, T. Esslinger, Nature (London) **455**, 204 (2008).

[5] M.P.A. Fisher, P.B. Weichman, G. Grinstein, and D.S. Fisher, Phys. Rev. B **40**, 546 (1989).

[6] D. Jaksch, C. Bruder, J.I. Cirac, C.W. Gardiner, and P. Zoller, Phys. Rev. Lett. **81**, 3108 (1998).

[7] L.M. Duan, E. Demler, and M.D. Lukin, **91**, 090402 (2003).

[8] B. Paredes, A. Widera, V. Murg, O. Mandel, S. Folling, I. Cirac, G.V. Shlyapnikov, T.W. Hansch, and I. Bloch, Nature (London) **429**, 277 (2004).

[9] T. Kinoshita, T. Wenger, and D.S. Weiss, Science **305**, 1125 (2004).

[10] M. Albiez, R. Gati, J. Folling, S. Hunsmann, M. Cristiani, and M.K. Oberthaler, Phys. Rev. Lett. **95**, 010402 (2005).

[11] See for example, T. Giamarchi, *Quantum Physics in One Dimension* (Oxford University Press, Oxford, 2004).

[12] K. Lanczos, J. Res. Natl. Bur. Stand **45**, 225 (1950).

[13] S.R. White, Phys. Rev. Lett. **69**, 2863 (1992); Phys. Rev. B **48**, 10345 (1993).

[14] K. Okunishi and T. Tonegawa, J. Phys. Soc. Jpn. **72**, 479 (2003).

[15] F. Heidrich-Meisner, A. Honecker, and T. Vekua, Phys. Rev. B **74**, 020403(R) (2006).

[16] T. Hikihara, T. Momoi, A. Furusaki, and H. Kawamura, Phys. Rev. B **81**, 224433 (2010).

[17] C. Holzhey, F. Larsen, and F. Wilczek, Nucl. Phys. B **424**, 443 (1994).

[18] P. Calabrese and J. Cardy, J. Stat. Mech.: Theory Exp. (2004) P06002.

[19] P. Jordan and E. Wigner, Z. Phys. **47**, 631 (1928).

[20] A.A. Nersesyan, A. O. Gogolin, and F.H.L. Essler, Phys. Rev. Lett. **81**, 910 (1999).

[21] P. Lecheminant, T. Jolicoeur, and P. Azaria, Phys. Rev. B **63**, 174426 (2001)

[22] A. Kolezhuk and T. Vekua, Phys. Rev. B **72**, 094424 (2005).

[23] I.P. McCulloch, R. Kube, M. Kurz, A. Kleine, U. Schollwock, and A.K. Kolezhuk, Phys. Rev. B **77**, 094404 (2008).

[24] K. Okunishi and T. Tonegawa, Phys. Rev. B **68**, 224422 (2003).

[25] J. Igarashi, J. Phys. Soc. Jpn. **58**, 4600 (1989).

[26] A.V. Chubukov, Phys. Rev. B **44**, 4693 (1991).

[27] T. Hikihara, L. Kecke, T. Momoi, and A. Furusaki, Phys. Rev. B **78**, 144404 (2008).

[28] S.R. White and I. Affleck, Phys. Rev. B **54**, 9862 (1996).

[29] T. Hikihara, M. Kaburagi, and H. Kawamura, Phys. Rev. B **63**, 174430 (2001).

[30] T. Giamarchi and A.J. Millis, Phys. Rev. B **46**, 9325 (1992); T. Giamarchi, Physica B **230-232**, 975 (1997).

[31] G. Gomez-Santos, Phys. Rev. Lett. **70**, 3780 (1993).